van Hove scenario and thermopower behavior of the high-T_c cuprates

G. C. McIntosh and A. B. Kaiser
Physics Department, Victoria University of Wellington, P.O. Box 600, Wellington, New Zealand
(Received 7 June 1996)

We examine the requirements for a van Hove singularity in the electronic density of states to cause the systematic thermopower behavior observed in the normal state of the cuprate superconductors. We concentrate on the Bi-, Tl-, and Hg-based cuprates which are not complicated by the presence of CuO chains and in which a wide range of doping levels can be achieved. Our calculations, using a simple model for the van Hove singularity, can reproduce the experimental data well, provided a wideband thermopower contribution is also present and provided the singularity remains close to the chemical potential as the carrier concentration varies. [S0163-1829(96)03541-2]

I. INTRODUCTION

The explanation of the electronic transport properties of the high-T_c superconductors remains controversial. For example, the experimental linearity of resistivity with temperature over a wide temperature range above T_c has been derived from several different theoretical models, such as those involving van Hove singularities,[1,2] spin fluctuations,[3,4] and bipolaronic superconductivity,[5] as well as electron-phonon mechanisms.[6]

One electronic transport property that appears very worthwhile investigating in the cuprates is thermoelectric power. Unlike the resistivity, the temperature dependence of thermopower does not depend explicitly on the temperature dependence of the carrier scattering rate. Metallic diffusion thermopower is, however, very sensitive to electronic structure, in particular to the location relative to the Fermi level of those electronic states contributing most to conduction. The normal-state thermopower would therefore be expected to provide a useful probe to test the van Hove scenario for high-temperature superconductors, in which high-T_c superconductivity is linked to the existence of van Hove singularities in the electronic density states close to the Fermi level.[7–9,1] Evidence for such singularities near the Fermi level in the high-T_c superconductors has been provided by angle-resolved photoemission[10,11] and by band-structure calculations.[12,13]

For most of the cuprate superconductors, a remarkable systematic thermopower pattern is observed.[14,15] In the underdoped regime, the in-plane thermopower typically exhibits a positive peak between $T\sim 50$ K and $T\sim 150$ K, decreasing approximately linearly with temperature at higher temperatures. With increasing carrier concentration, the thermopower shifts to lower values with the slope being approximately independent of doping level. Finally, in the overdoped regime, the thermopower becomes negative and the approximately linear decrease with temperature is reminiscent of metallic diffusion thermopower. A trend observed in many cuprates is that the room temperature thermopower is approximately zero[16] for optimally doped samples with maximum T_c.

The negative temperature coefficient of cuprate thermopower is less systematic in the $YBa_2Cu_3O_{7-y}$ family, particularly in optimally or slightly overdoped samples, but these materials are complicated by the presence of CuO chains that contribute to conduction along one of the plane directions. Measurements on untwinned crystals by three different groups[17] show that negative slopes are observed for in-plane conduction perpendicular to the CuO chains, indicating that this is the standard pattern associated with the CuO_2 planes.

In this paper, we investigate the extent to which this standard thermopower temperature dependence is consistent with the van Hove scenario. Early calculations of the transport properties of $YBa_2Cu_3O_{7-y}$ for a nearest-neighbor tight-binding model involving a van Hove singularity[18] showed how a very narrow peak almost at the Fermi level could produce an approximately constant thermopower for temperatures of the order of the width of the peak. Newns *et al.*[19] showed how the variation of the Fermi level through a logarithmic van Hove singularity in the density of states could reproduce the general thermopower behavior of $YBa_2Cu_3O_{7-y}$ as oxygen depletion y varied. In particular, the change in sign of the thermopower as a function of y near the value for maximum T_c corresponded to the Fermi level passing the peak of the singularity. Our early calculations[20] using a logarithmic singularity superimposed on a linearly varying density of states yielded positive peaks in the thermopower with decreases at higher temperatures.

In this paper, our investigation of the standard thermopower pattern in the van Hove singularity scenario also focuses on the changes in sign of the thermopower as a function of temperature, which has not previously been analyzed. To do this, we make a detailed comparison of simple model calculations with recent thermopower measurements[21–23] in the Bi-, Tl-, and Hg-based cuprate superconductor series in which the doping level can be varied from underdoped to overdoped.

We find that the standard thermopower temperature dependence is generally consistent with the van Hove scenario but that, in addition to a sharp feature in the density of states, an extra wideband thermopower contribution is required to account for the linear negative slope at higher temperatures, and also that the van Hove singularity must be pinned near the Fermi level as the doping level varies in order to give the thermopower peaks observed.

II. THERMOPOWER MODEL

To investigate the van Hove scenario, we use the standard expression for diffusion thermopower,[24,25]

$$S=\frac{1}{eT\sigma}\int(\varepsilon-\mu)\sigma(\varepsilon)\frac{\partial f_0}{\partial\varepsilon}d\varepsilon, \tag{1}$$

where the conductivity is expressed in terms of a partial conductivity function $\sigma(\varepsilon)$ at energy ε:

$$\sigma=-\int\sigma(\varepsilon)\frac{\partial f_0}{\partial\varepsilon}d\varepsilon. \tag{2}$$

Here μ is the chemical potential, f_0 is the Fermi-Dirac function, $\partial f_0/\partial\varepsilon$ is the Fermi window function, and e is the electronic charge.

It is seen that it is the shape of $\sigma(\varepsilon)$ as a function of energy, in particular the relative asymmetry of the energy dependence of $\sigma(\varepsilon)$ about the Fermi level, that is the crucial factor in determining thermopower. Hence we seek to determine what shape, if any, can account for the observed thermopower pattern in the cuprates, focusing on the effect of a van Hove singularity in the density of states without assuming any particular scattering mechanism for the carriers. As a simple starting point, we consider a two-dimensional nearest-neighbor tight-binding (NNTB) dispersion relation, given by[18]

$$\varepsilon=\frac{W}{4}(\cos k_x a+\cos k_y a), \tag{3}$$

where W is the bandwidth and k_x and k_y are the wave vectors in the CuO_2 planes. This gives a logarithmic van Hove singularity in the density of states $N(\varepsilon)$:

$$N(\varepsilon)=\frac{1}{2\pi^2}\int\frac{dS}{\|\nabla_k\varepsilon\|} \tag{4}$$

(where $\nabla_k\varepsilon$ is the gradient of the ε vs $\mathbf{k}$ dispersion relation), and a sharp cusp in $\sigma(\varepsilon)$, calculated from[18]

$$\sigma(\varepsilon)=\frac{e^2\Lambda}{4\pi^2c\hbar}\int d\Gamma \tag{5}$$

for a system of conducting planes where c is the lattice constant between adjacent planes, $\int d\Gamma$ is an integral over constant energy contours of the ε vs $\mathbf{k}$ dispersion relation in two-dimensions, and Λ is the quasiparticle mean free path. The energy dependence of Λ within the Fermi window is neglected for the present.

We follow Penn and Cohen[26] by ''smearing out'' narrow band singularities by applying a Lorentzian convolution to simulate disorder and inhomogeneity in the system, which would be likely to smear out sharp features in the density of states. The resulting peaks in $N(\varepsilon)$ and the partial conductivity function $\sigma(\varepsilon)$ are illustrated by the narrow band contributions in Fig. 1.

The above narrow band density of states and partial conductivity function are symmetric about the middle of the band, and so the thermopower is zero when the chemical potential coincides with the middle of the band. Fortunately, the temperature dependence of thermopower is determined only by the shape of $\sigma(\varepsilon)$ and is independent of the temperature dependence of the mean free path Λ, since the constants in Eq. (5) cancel from the numerator and denominator of Eq. (1). It is, however, necessary in general to take account of the temperature dependence of the chemical potential $\mu(T)$, which is calculated self-consistently for a constant carrier concentration n by using

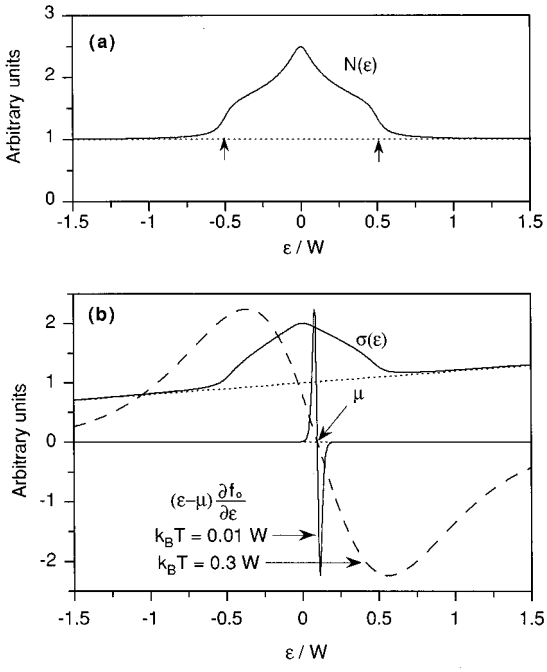

FIG. 1. (a) Model density of states $N(\varepsilon)$, consisting of a narrow band (of width W indicated by the arrows) with a broadened van Hove singularity at the center, and a two-dimensional wide band (dotted line). (b) Partial conductivity $\sigma(\varepsilon)$ derived from the density of states in (a) for a conductivity weighting factor $r\simeq 0.5$ (see text), together with the thermopower weighting factor $(\varepsilon-\mu)(\partial f_0/\partial\varepsilon)$ at low and high temperatures.

$$n=\int N(\varepsilon)f_0(\varepsilon)d\varepsilon. \tag{6}$$

If we consider the thermopower due to a single narrow band only, above half filling (as shown by Bar-ad *et al.*[18] and reproduced by our calculations) the symmetric narrow band density of states can give a small thermopower peak as temperature increases, followed by a plateau and gradual increase to the saturation value given by

$$S=\left(\frac{k}{e}\right)\ln\left(\frac{n_f}{1-n_f}\right), \tag{7}$$

where n_f is the fractional occupancy of the narrow band. The behavior for less than half filling is the mirror image with negative values. In the presence of a mobility edge, a thermopower decreasing in magnitude can be obtained,[18] but again the model does not give the change of sign as temperature increases, seen in experiments[21–23] on the Bi-, Tl-, and Hg-based cuprate superconductors.

Our calculations can also give a thermopower decreasing in magnitude above the peak in S vs T (either positive or negative) if the chemical potential is held fixed, as for the

behavior calculated by Newns *et al.*[19] for a logarithmic density of states. In this case, also, the thermopower does not change sign as a function of temperature. To achieve this change of sign within the van Hove scenario, asymmetry is required. To incorporate this asymmetry within the narrow band, we have tried calculations including interactions beyond nearest neighbors in a two-dimensional tight-binding model, which leads to asymmetry in the density of states,[27] and confirmed that this asymmetry can produce a change in sign of thermopower with temperature. However, these calculations have been unable to reproduce systematically the linearity of high-temperature thermopower over a range of doping levels, as seen experimentally. We therefore do not consider this case further.

In order to get a thermopower which decreases at higher temperatures with a possible change of sign and also exhibits the linear metalliclike behavior at high temperatures, especially in the overdoped regime, it appears a normal linear metallic diffusion thermopower contribution is needed. This corresponds to a linear term in $\sigma(\varepsilon)$ extending across the Fermi window, as in the standard model for metallic diffusion thermopower and shown by the dotted line in Fig. 1(b). For a two-dimensional free electron band there would be a corresponding constant term in the density of states, as in Fig. 1(a).

Our model shown in Fig. 1 is the simplest representation we can give to account for the data of what is inevitably a more complex situation. The consistency of the thermopower pattern for different cuprate superconductors does, however, suggest a relatively simple underlying origin rather than a sensitivity to the details of each material. The essential features are a normal metallic wideband contribution as well as a relatively narrow peak in the partial conductivity (of total width W) near the Fermi level, which seems plausible in the light of band-structure calculations.[12,13] We have calculated this peak in $\sigma(\varepsilon)$ for a particular narrow band with a broadened van Hove singularity at the center, but our analysis is more generally applicable.

If the relaxation time $\tau(\varepsilon)$ has a strong energy dependence near the singularity, as in the marginal Fermi liquid model where $\tau(\varepsilon)\propto 1/\varepsilon$ at small energies for $\mu=0$, the effect is merely to change the density of states required within the narrow band to give the partial conductivity shown in Fig. 1(b), without a major qualitative change in the model. This is confirmed by the fact that our model gives a similar pattern to that of Newns *et al.*[19] in the absence of a wideband energy dependence in $\sigma(\varepsilon)$, as shown by calculations to fit the Hg1223 data below. A strong energy dependence of the relaxation time that is asymmetric about the chemical potential can affect thermopower substantially, as in magnetic materials, but the regularity of the thermopower behavior seen in widely varying cuprate superconductors argues against the significance of this effect.

The basic idea as to how the partial conductivity function of Fig. 1(b) gives the type of thermopower behavior seen in the data can be seen as follows. As seen from Eq. (1), the thermopower is governed by the overlap between the partial conductivity $\sigma(\varepsilon)$ and the antisymmetric Fermi-window function $(\varepsilon-\mu)(\partial f_0/\partial\varepsilon)$, which is sketched in Fig. 1(b) at high temperatures (dashed line) and low temperatures (solid line) for the case where the Fermi level is just above the van Hove singularity. At low temperatures the Fermi window is very narrow and S indicates the slope of $\sigma(\varepsilon)$ in the vicinity of μ. In Fig. 1(b), S is positive at low temperatures since $\sigma(\varepsilon)$ has greater magnitude beneath the positive peak of $(\varepsilon-\mu)(\partial f_0/\partial\varepsilon)$. As the temperature increases, the Fermi window spreads out so that the positive peak in $(\varepsilon-\mu)(\partial f_0/\partial\varepsilon)$ passes over the cusp in $\sigma(\varepsilon)$. This gives rise to a peak in S vs T. At higher temperatures the narrow band becomes of less significance within the width of the Fermi window. The thermopower will then become dominated by the wide band with its positive slope in $\sigma(\varepsilon)$, and so commence decreasing towards a negative value.

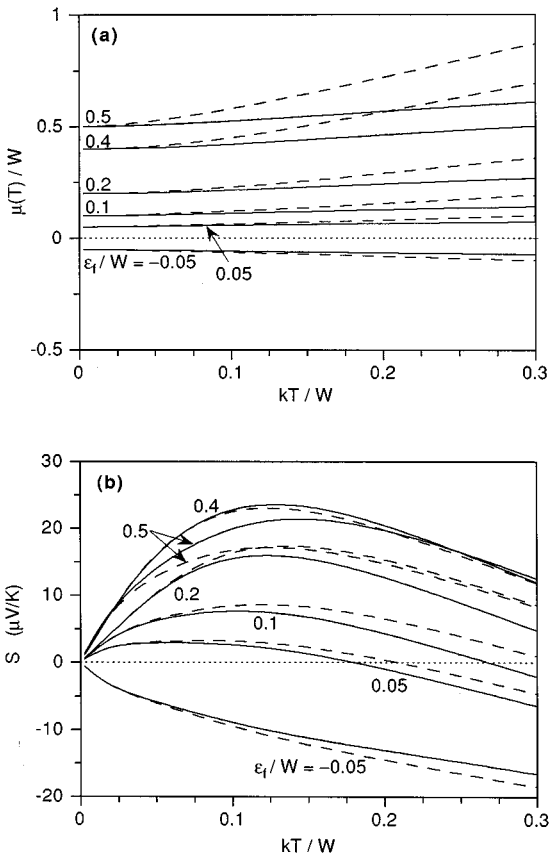

FIG. 2. Calculated temperature dependence of (a) the chemical potential $\mu(T)$ and (b) the thermopower S for various positions of the normalized Fermi energy $\varepsilon_f=\mu(0)/W$ relative to the narrow band center. The solid lines are for a conductivity weighting factor $r\simeq 0.5$ for the narrow band relative to the wide band, and the dashed lines are for $r\simeq 0.05$ (see text).

This pattern is illustrated by typical results obtained from this model shown in Fig. 2, which were calculated for the partial conductivity function $\sigma(\varepsilon)$ shown in Fig. 1(b) for varying locations of the Fermi level ε_f with respect to the narrow band peak. The magnitude of the thermopower is controlled by the position of the Fermi level. As ε_f gets close to the narrow band peak, the thermopower peak moves to lower temperatures and diminishes in size, since the positive peak of $(\varepsilon-\mu)(\partial f_0/\partial\varepsilon)$ passes the narrow band peak at lower temperatures. Note that when the Fermi level is below the peak, it causes a negative contribution to thermopower, and so the combined effect of the narrow band peak and the wide band leads to negative thermopowers at all temperatures, as shown in Fig. 2(b).

For the partial conductivity function of Fig. 1(b), $\varepsilon_f/W \simeq 0.4$ gives the maximum obtainable thermopower of $S \sim 25\mu \mathrm{V\,K}^{-1}$, as shown in Fig. 2(b). For $\varepsilon_f/W > 0.4$ the peak magnitude of S decreases again because, as ε_f increases further, the chemical potential approaches and enters the wideband region and the narrow band has progressively less effect on thermopower. Larger thermopower peaks can be obtained if there is more weight in the peak in $\sigma(\varepsilon)$.

Although we can regard our partial conductivity $\sigma(\varepsilon)$ function in Fig. 2 as a generic shape that directly determines thermopower through Eqs. (1) and (2), we need to consider the density of states explicitly in order to calculate the temperature dependence of the chemical potential $\mu(T)$ from Eq. (6). This introduces a degree of dependence on specific model parameters that give the relative narrow band and wideband contributions to conductivity. For example, the density of states in Fig. 1(a) corresponds to a conductivity weighting factor $r \simeq 0.5$, where r is defined as the average contribution of the narrow band to conductivity relative to the wide band, over the width of the narrow band. This means that the integrated relative peak in the $\sigma(\varepsilon)$ is half that in $N(\varepsilon)$, corresponding for example to somewhat lower mobility in the narrow band.

The temperature dependence of $\mu(T)$ is of paramount importance where there is only the narrow band with no wideband contribution: For this case, the temperature dependence of $\mu(T)$ strongly affects thermopower, which, for example, saturates[18] rather than decreases as temperature increases. However, this is not true for the cases we consider. To show the effect of variations in this ratio r, we plot in Fig. 2 the temperature dependence of the chemical potential and thermopower for $r \simeq 0.05$ (dashed lines) as well as for $r \simeq 0.5$ (solid lines). The differences even for this large change in r are not great, showing that our calculations are not crucially dependent on the value of this parameter. For larger relative contributions to conductivity from the narrow band ($r > 1$), the change from the $r \simeq 0.5$ curves is very small, because the chemical potential is largely determined by the wideband states and as typical in that case shows an even smaller temperature dependence.

III. COMPARISON WITH EXPERIMENT

As mentioned above, a large body of data indicates a systematic pattern for the in-plane thermopower temperature dependence in cuprate superconductors.[14,15] The best examples for comparison with calculations are those where the doping levels can be varied over a wide range to show the shift of thermopower with carrier concentration. Fits of our model to experimental thermopowers[21–23] are given for the Bi2201 series in Fig. 3, the Tl1201 series in Fig. 4, annealed Hg1201 samples in Fig. 5, and Hg1223 in Fig. 6. The fitted parameter values are given in Table I (the thermopower is zero in the superconducting state, and so the fits are for temperatures above the fluctuation regime).

It can be seen that our model is very capable of reproducing global trends seen in the experimental thermopower data such as the positive peak in the thermopower in the underdoped regime, the decrease in thermopower with increased hole concentration, the change in sign of thermopower seen at intermediate doping levels, and the approximately linear decrease with temperature in the overdoped regime.

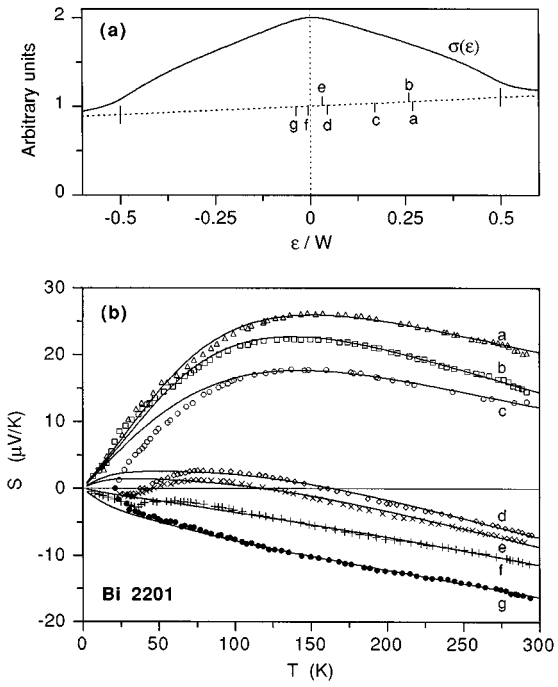

FIG. 3. Fits of our model to the thermopower data of Subramaniam *et al.* (Ref. 21) for the $Bi_2Sr_{2-x}La_xCuO_{6+y}$ (La-doped Bi2201) series of superconductors as the hole concentration is increased from underdoped (sample a) to overdoped (sample g). The position of the Fermi level relative to the narrow band for each fit is shown in (a), and the corresponding fits to the data in (b). Fit parameters are listed in Table I.

There is essentially no difference in the calculated fit curves for conductivity weighting factors $r \simeq 0.5$ and $r \simeq 0.05$, except for the Hg1223 case where T_c is very large and the peak must occur below T_c. The differences in the fitted bandwidth W for the two values of r are $\simeq$ 2% for Tl1201, 7% for Bi2201, 18% for Hg1201, and 28% for Hg1223, with corresponding variations in E_f. The greater difference for the Hg-based materials reflects the fact that

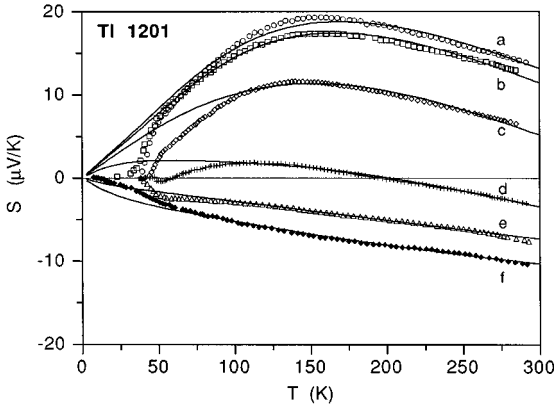

FIG. 4. Fits of our model to the thermopower data of Subramaniam *et al.* (Ref. 21) for the $Tl_{0.5}Pb_{0.5}Sr_{2-x}La_xCuO_5$ (La-doped Tl1201) series as hole concentration increases (samples $a \rightarrow f$). Fit parameters are listed in Table I.

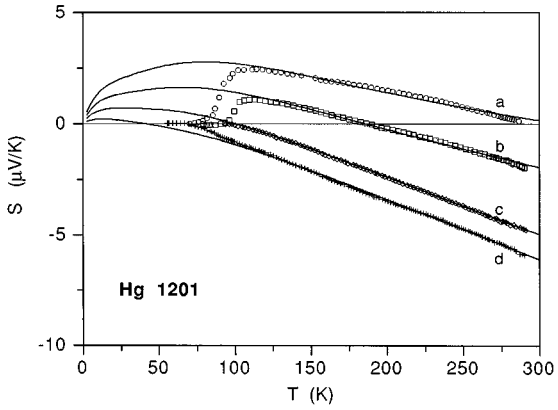

FIG. 5. Fits of our model to the thermopower data of Subramaniam *et al.* (Ref. 22) for the $HgBa_2CuO_{4+y}$ (Hg1201) series as hole concentration increases (samples $a \rightarrow d$). Fit parameters are listed in Table I.

their peak in S vs T is suppressed below $T = T_c$ and so is inaccessible to our fitting procedures. Overall, we conclude that the temperature dependence of the chemical potential is not too significant in our model and list only the values for $r \simeq 0.5$ in Table I.

The relative size of the peak in $\sigma(\varepsilon)$ was taken as the same in all cases, i.e., with equal contributions from the narrow band and wide band at the midpoint of the narrow band. This peak reproduces the size of the experimental thermopower, but similar fits can also be obtained for larger peaks with smaller values of ε_f.

The width W of the narrow band peak in $\sigma(\varepsilon)$ was held fixed for all members of the same series. The changing thermopower then arises largely from the lowering of the Fermi level ε_f as the hole concentration is increased, as shown explicitly for the Bi2201 series in Fig. 3(a). Our fits do indicate the width of the narrow band peak in $\sigma(\varepsilon)$, which controls the position (with temperature) of the peak in our theoretical S vs T graphs. Typically, the narrow band width is

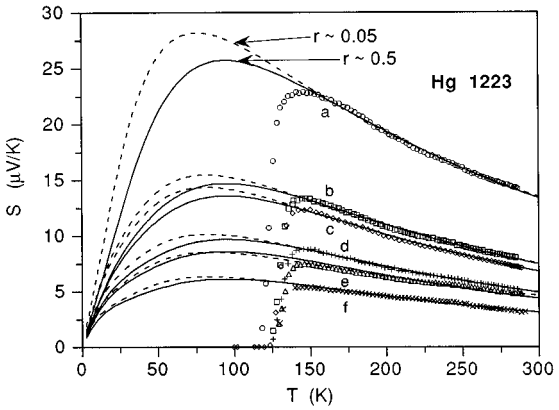

FIG. 6. Fits of our model to the thermopower data of Subramaniam *et al.* (Ref. 23) for the $Hg_{0.5}Ba_2Ca_2Cu_3O_{8+y}$ (Hg1223) series as hole concentration increases (samples $a \rightarrow f$). Fit parameters for conductivity weighting factor $r \simeq 0.5$ (solid lines) are listed in Table I; for comparison, fits for $r \simeq 0.05$ (dashed lines) are also shown.

TABLE I. Fit parameters for the fits of our model to thermopower data shown in Figs. 3 – 6, for a conductivity weighting factor $r \simeq 0.5$. W is the width of the narrow band, ε_f the Fermi energy relative to the center of the narrow band, and α the temperature coefficient of the linear thermopower due to the wide band alone.

Data set		W (eV)	E_f (eV)	α (μV K^{-2})
Bi2201	(a)	0.085	0.023	−0.001
	(b)		0.022	−0.025
	(c)		0.015	−0.013
	(d)		0.0039	−0.058
	(e)		0.0027	−0.058
	(f)		−0.0004	−0.054
	(g)		−0.0032	−0.062
Tl1201	(a)	0.124	0.036	−0.054
	(b)		0.034	−0.058
	(c)		0.022	−0.062
	(d)		0.0054	−0.046
	(e)		−0.0014	−0.032
	(f)		−0.0042	−0.034
Hg1201	(a)	0.050	0.0012	−0.006
	(b)		0.00086	−0.013
	(c)		0.00058	−0.025
	(d)		0.00029	−0.028
Hg1223	(a)	0.053	0.014	0.000
	(b)		0.0067	0.000
	(c)		0.0062	0.000
	(d)		0.0042	0.000
	(e)		0.0037	0.000
	(f)		0.0026	0.000

required to be of the order of $W \sim 0.05 - 0.1$ eV, the smaller values being for the Hg-based superconductors since the peak is at lower temperatures than in the Bi2201 and Tl1201 series.

The α parameter represents the temperature coefficient of the thermopower in the high-temperature limit, and is determined solely by the wideband contribution to $\sigma(\varepsilon)$. The value of α is consistently negative, reflecting the standard pattern of cuprate thermopower,[14,15] but is very small in the Hg1223 series.

At this stage our model is too simple to reproduce the dip in S vs T just above T_c seen in the experimental data for Bi2201 (Fig. 3) near optimal doping. However, we note that this feature could be produced by a small subsidiary peak in $\sigma(\varepsilon)$ just above the Fermi level, as in Fig. 7. The sharp feature would need to be pinned above the Fermi level to produce the effect in both samples c and d.

IV. DISCUSSION

It is clear from the fits to the data in Figs. 3–6 that our simple model can account well for the systematic thermopower behavior of the cuprate superconductors if there is a peak in the partial conductivity $\sigma(\varepsilon)$ of width $W \sim$ 0.05–0.1 eV such as might be produced by a van Hove singularity in the density of states. Other thermopower data for the cuprates are also consistent with this picture.[28] Calculations by

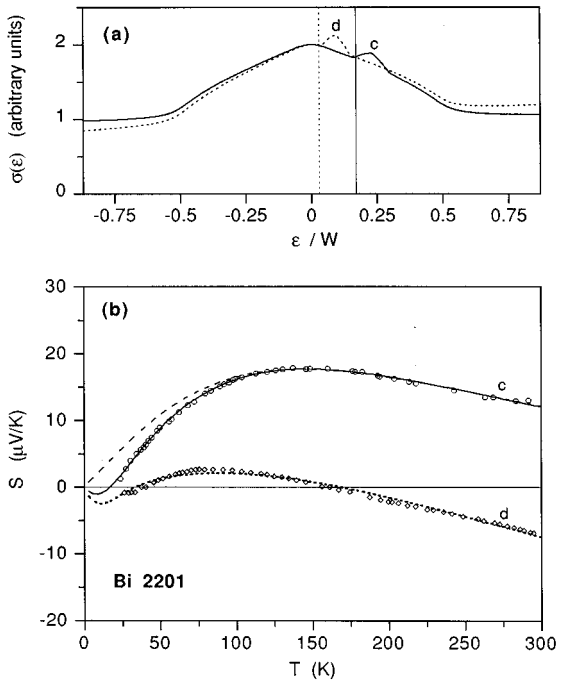

FIG. 7. Illustration that an extra small peak in the narrow band density of states (a) can account for the dip in thermopower seen at low temperatures in Bi2201 samples. The location of the Fermi level is indicated by the corresponding vertical line (solid or dotted) in (a), and the corresponding fits are shown in (b) (the previous fit for sample c from Fig. 3 is also shown as the dashed line for comparison).

Novikov and Freeman[13] for Hg-based cuprates give valence bands extending over an 8 eV region, with narrow van Hove peaks of width of approximately 0.2 eV that coincide with the Fermi level upon doping with 0.4–0.6 holes per formula unit.

Thus the picture we infer from fits to experimental data does not appear too unreasonable. We stress that for the model to work we do require a wide linear band in conjunction with a sharp feature in the density of states. This is necessary to have a metalliclike thermopower in the overdoped regime, a peak in the thermopower in the underdoped regime, and a thermopower which changes sign at intermediate doping levels. Obviously, if the proximity of the Fermi level to the van Hove singularity is associated with the high T_c, the model yields the trend whereby the thermopower changes sign near optimal doping, as discussed by Newns *et al.*[19]

Another requirement in our model is that the Fermi level must lie within the narrow band for the superconducting regime and so some sort of pinning mechanism is required. We also note that a small splitting of the van Hove peak was calculated by Novikov and Freeman[13] for Hg1201 and Hg1212. This would not be likely to produce observable effects in thermopower above T_c for these materials, but more effect on thermopower would be found if a similar splitting occurred for superconductors such as Bi2201 and Tl1201 with lower T_c. Nevertheless, an explanation of the thermopower behavior shown in Fig. 7 remains very speculative because of the required pinning of the subsidiary peak above the Fermi level.

One feature of the cuprate thermopower pattern not addressed directly by the van Hove scenario is the lack of symmetry in the occurrence of positive and negative thermopower peaks seen in the experimental data and also the lack of symmetry in resistivity magnitude, corresponding to the Fermi level on either side of the van Hove peak. It appears that other factors, for example the tendency to localization in the underdoped regime, need to be taken into account.

We also note that there are other mechanisms that could produce behavior resembling the systematic experimental thermopower pattern, such as phonon drag[14,29] and the electron-phonon renormalization of metallic diffusion thermopower.[30]

ACKNOWLEDGMENTS

G.C.M. would like to thank the Victoria University of Wellington Scholarships Committee for financial support. A.B.K. thanks Bertina Fisher for helpful discussions, C.C. Tsuei for sending copies of his papers, and the New Zealand Foundation for Research, Science and Technology for partial support.

[1] D. M. Newns, H. R. Krishnamurthy, P. C. Pattnaik, C. C. Tsuei, C. C. Chi, and C. L. Kane, Physica B **186-188**, 801 (1993).
[2] C. C. Tsuei, Physica A **168**, 238 (1990).
[3] P. Monthoux and D. Pines, Phys. Rev. B **49**, 4261 (1994).
[4] A. B. Kaiser, Philos. Mag. B **65**, 1197 (1992).
[5] David Emin, Phys. Rev. B **45**, 5525 (1992).
[6] R. Zeyher, Phys. Rev. B **44**, 10 404 (1991).
[7] J. Labbe and J. Bok, Europhys. Lett. **3**, 1225 (1987).
[8] J. Friedel, J. Phys. Condens. Matter **1**, 7757 (1989).
[9] R. S. Markiewicz, J. Phys. Condens. Matter **2**, 665 (1990).
[10] D. M. King, Z. X. Shen, D. S. Dessau, D. S. Marshall, C. H. Park, W. E. Spicer, J. L. Peng, Z. Y. Li, and R. L. Greene, Phys. Rev. Lett. **73**, 3289 (1994).
[11] K. Gofron, J. C. Campuzano, A. A. Abrikosov, M. Lindroos, A. Bansil, H. Ding, D. Koelling, and B. Dabrowski, Phys. Rev. Lett. **73**, 3302 (1994).
[12] Warren E. Pickett, Rev. Mod. Phys. **61**, 433 (1989).
[13] D. L. Novikov and A. J. Freeman, Physica C **216**, 273 (1993).
[14] A. B. Kaiser and C. Uher, in *Studies of High Temperature Superconductors*, edited by A.V. Narlikar (Nova Science, New York, 1991), Vol. 7, p. 353.
[15] A. B. Kaiser, C. K. Subramaniam, B. Ruck, and M. Paranthaman, Synth. Met. **71**, 1583 (1995).
[16] S. D. Obertelli, J. R. Cooper, and J. L. Tallon, Phys. Rev. B **46**, 14 928 (1992).
[17] C. K. Subramaniam, H. J. Trodahl, A. B. Kaiser, and B. J. Ruck, Phys. Rev. B **51**, 3116 (1995).
[18] S. Bar-ad, B. Fisher, J. Ashkenazi, and J. Genossar, Physica C **156**, 741 (1988).

[19] D. M. Newns, C. C. Tsuei, R. P. Huebener, P. J. M. van Bentum, P. C. Pattnaik, and C. C. Chi, Phys. Rev. Lett. **73**, 1695 (1994).
[20] K. E. J. Goh and A. B. Kaiser (unpublished).
[21] C. K. Subramaniam, C. V. N. Rao, A. B. Kaiser, H. J. Trodahl, A. Mawdsley, N. E. Flower, and J.L. Tallon, Supercond. Sci Technol. **7**, 30 (1994).
[22] C. K. Subramaniam, M. Paranthaman, and A. B. Kaiser, Physica C **222**, 47 (1994).
[23] C. K. Subramaniam, M. Paranthaman, and A. B. Kaiser, Phys. Rev. B **51**, 1330 (1995).
[24] J. S. Dugdale, *The Electrical Properties of Metals and Alloys* (Edward Arnold, London, 1977), p. 106.
[25] Philip B. Allen, W. E. Pickett, and H. Krakauer, Phys. Rev. B **37**, 7482 (1988).
[26] D. R. Penn and Marvin L. Cohen, Phys. Rev. Lett. **46**, 5466 (1992).
[27] M. J. Lercher and J. M. Wheatley, Physica C **215**, 145 (1993).
[28] G. C. McIntosh (unpublished).
[29] C. Uher, A. B. Kaiser, E. Gmelin, and L. Walz, Phys. Rev. B **36**, 5676 (1987); H.J. Trodahl, *ibid.* **51**, 6175 (1995).
[30] A. B. Kaiser and G. Mountjoy, Phys. Rev. B **43**, 6266 (1991).